

**2016 NDIA GROUND VEHICLE SYSTEMS ENGINEERING AND TECHNOLOGY
SYMPOSIUM
MODELING & SIMULATION, TESTING AND VALIDATION (MSTV) TECHNICAL SESSION
AUGUST 2-4, 2016 - NOVI, MICHIGAN**

**THE DEVELOPMENT OF A FLOORING SYSTEM FOR INJURY MITIGATION
AND STRUCTURAL ISOLATION IN UNDERBELLY BLAST EVENTS**

Kevin Kwiatkowski
Pratt & Miller Engineering
New Hudson, MI

Christopher Watson
Pratt & Miller Engineering
New Hudson, MI

Chantelle Korson
US Army TARDEC
Warren, MI

ABSTRACT

The CAMEL program focused on force protection and demonstrated the possibility to protect occupants through higher underbelly blast levels than normally or previously observed. This required a holistic vehicle systems engineering approach to mitigate blast injuries that both optimized existing systems as well as developed new technologies. The result was zero injury to all occupants as assessed by 5th, 50th, and 95th percentile encumbered ATDs during survivability blast testing. Twelve full scale objective-level blast tests were performed on over seventy fully-instrumented ATDs without a single lower-extremity injury. The lower limb protection was provided by an isolated floor system. This system was developed from the ground-up and occupant-out during the CAMEL program. This paper chronicles the CAMEL floor system's creation, design, testing, and development process.

INTRODUCTION

Tibia and lower leg injuries are a major concern in underbody blast events. Approximately one third of all soldiers injured in underbody blast events sustain foot/ankle fractures or tibia/fibula fractures [1]. Worse yet, many of these injuries are severe enough that they lead to amputation or permanent disabilities.

Modern hull technologies have enabled vehicle structures to survive blast events large enough to cause lower extremity injuries. This has required the vehicle to mitigate the blast event externally through modern hull technology, along with limiting the energy transmitted through the occupants internally for injury mitigation. Integrating the internal structure of the vehicle to become an energy absorption device requires a ground up vehicle design effort.

Historic underbelly blast survivability testing utilizes the Army Research Lab / Survivability / Lethality / Analysis Directorate (ARL/SLAD) requirements that consider only 50th percentile Anthropomorphic Test Devices (ATDs), representing a 50th percentile male. As the clean-sheet design in the Occupant Centric Platform, Technology Enabled Capability Demonstrator (OCP-TECD), the Concept for Advanced Military Explosion-mitigating Land

demonstrator (CAMEL) program is the first full testing regimen to include the 5th, 50th, and 95th percentile test devices. This represents a wider cross-section of the soldier population and also presents unique challenges.

Current flooring system technologies are dominantly applique solutions, generally set atop the existing rigid walking floor. Blast mats are the leading injury mitigation device employed in both the research community and fielded vehicles. Multiple commercially available mats are shown in Figure 1. They are very effective for limiting load through small impulse events and removing low energy shock and high frequency content. This technology was deemed inadequate on its own during the large CAMEL objective blast levels. The final CAMEL floor system solution did utilize a blast mat as part of the system function, located atop the stroking floor system.

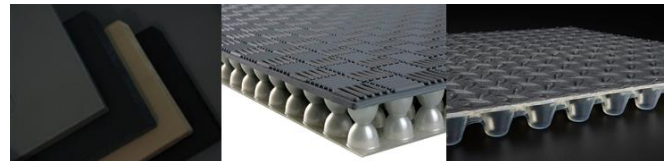


Figure 1: Commercially available blast mats

DIFFERENCES: CAMEL APPROACH VS LEGACY

CAMEL and OC (Occupant Centric) requirements introduced more challenging occupant protection standards than the conventional ARL/SLAD evaluation criteria. The most significant change was assessing injury for the 5th, 50th, and 95th percentile ATD sizes instead of just the 50th. Leg mass varies dramatically from the 5th to 50th to 95th occupants. While proportionally similar, the tibia injury threshold does not scale linearly along with mass it supports. This results in slightly different optimum leg accelerations for all occupants, but widely differing foot input loads to the flooring system. The governing static solution physics indicating the optimum floor accelerations and imparted loads are shown in Table 1. This data indicates a constant acceleration floor system should perform well, but its response must be intrinsic and not impacted by seating positions or mass of the occupants.

		5th Percentile Female	50th Percentile Male	95th Percentile Male
Lower Leg Mass	[kg]	5.6	9.6	11.4
PPE Mass	[kg]	3.1	3.3	3.5
Lower Leg Mass w/PPE	[kg]	8.7	12.9	14.9
Foot to Floor Loading (normalized)	[N]	72%	100%	119%
Peak Calculated Leg Acceleration (normalized)	[G]	107%	100%	103%
Total ATD Mass w/ PPE	[kg]	75.8	106.9	132.7

Table 1: ATD leg acceleration and floor loading

To further challenge the CAMEL program, the assets were subjected to multiple blast locations to further emphasize the realities of the war fighter in hazardous environments. The asset was subjected to worst-case blast positions including center, offset, and end blast locations while program criteria maintained all injury thresholds had to be met.

CAMEL VEHICLE AND FLOOR ARCHITECTURE

The simplest and most reliable method to achieve consistent floor system acceleration and reduce sensitivity to the number and types of occupants is to reduce their percentage influence on the floor mass. To accomplish this, the CAMEL vehicle architecture was influenced by the floor system. The seats were mounted on the floor system and multiple vehicle required components were also mounted within the floor system, underneath the walking floor surface. The deep V-hull layout reduces impulse during blast and also creates a healthy space claim for the floor system and mounting components within it.

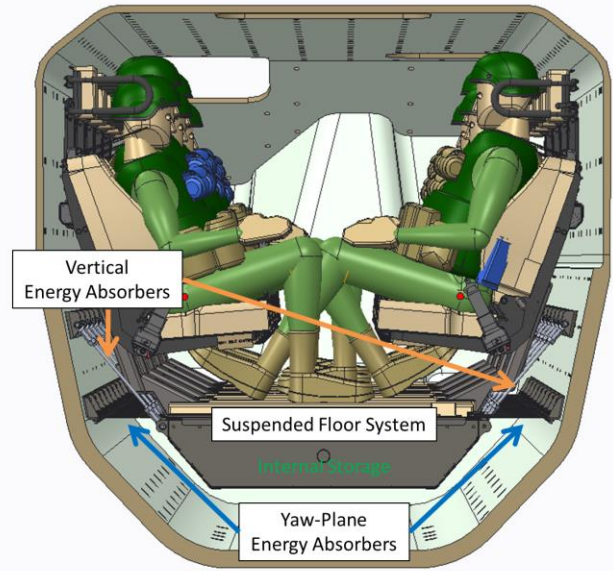


Figure 2: CAMEL vehicle and floor architecture

The floor Energy Absorber (EA) device design constraints were developed to maximize reliability and minimize time to potentially field a system. High performance was achieved with all passive stainless EA components that are easily manufactured with readily available materials. EA components were manufactured out of stainless due to its high specific toughness and strain rate sensitivity. Understanding and properly modeling strain rate sensitivity is imperative due to the duration of the blast event. A system conceptual constraint that was maintained throughout is floor protection must not be influenced by occupant foot placement. The entire floor load deck offers occupant protection during both the primary blast event as well as the subsequent return to ground event. The EA components were also designed to survive a full regimen of vehicle road loads.

To provide the additional protection required within the CAMEL program, a stroking floor system was developed. It moves a minimal amount during a blast event to limit acceleration to the lower extremities. It also mounts the squad seating system and multiple vehicle components to achieve a high floor mass and neutral response to vehicle loadout without impacting overall vehicle mass. It is suspended from vertical EA devices and uses yaw-plane absorbers that maintain lateral and longitudinal control while allowing the walls to resonate. It works during a centered blast and any offset blast locations. It removes local effects from the hull and acts as its own separate, isolated pod. Unlike traditional floor designs where the floor input is usually highest to the occupant seated directly above the blast, in this design, the floor output is relatively insensitive

to the location of the occupant in the floor. This floor system was developed through detailed explicit finite element modeling coupled with extensive laboratory and underbelly survivability blast testing. The full squad flooring system finite element model is shown in Figure 3.



Figure 3: CAMEL floor system FEA model

The CAMEL floor EA functions were split into two categories, yaw-plane and vertical support. The yaw-plane EA devices provide lateral and longitudinal support with a purposefully low vertical floor EA contribution. This allowed separate tuning for vertical EA performance. Initial calculations focused on the primary vertical EA performance during the blast pulse. Industry research uncovered many studies chronicling the performance of various EA devices. While no designs were directly applied, the concepts described in [1] were particularly insightful. The initial vertical EA device design direction involved two competing concepts, a constant force EA device paired against a variable force EA device.

The CAMEL program's constant force EA device featured a straight stainless rod that maintained a constant cross section throughout the active length of the EA device. The CAMEL program's variable force EA device was made out of stainless flat plate in the shape shown Figure 4, creating a "C" shape throughout the active EA area.



Figure 4: Vertical energy absorbing devices

The vertical EA devices were mounted above the floor, leaving the floor to hang below. By doing so, this creates a beneficiary motion ratio advantage during the blast event. The harsh lateral vibrations during the breathing of the hull structure are reduced by the advantageous lateral motion ratio, limiting the force transmitted into the floor.

PERFORMANCE TARGET SETTING EVOLUTION

Efforts were made to capture every feasible component and loading situation possible during the target setting phase. Systems engineering was employed with top level system performance targets feeding down to subsystem and component level specifications.

Anecdotal feedback from previous testing indicated the return to ground event was generally non-injurious and any injury experienced was predominantly during the primary blast pulse. The strategy for managing the return to ground pulse was to include a blast mat and evaluate severity after testing. This required the EA floor to maintain its integrity throughout the primary blast event, as well as return to ground.

All systems had to survive vehicle road loads that would be expected for the modern war fighter, which can be severe during vehicle off-road usage. Vertical accelerations in the 5G range can be experienced, as well as severe longitudinal and lateral loads on rough terrain. This developed a need for an in-plane EA device that could both survive road loads and keep the floor lateral and longitudinal motions under control during a blast event, including any extraneous wall motion and vibrations.

The first level of EA performance target setting utilized base physics and hand calculations. Vehicle footprint requirements were determined by floor acceleration performance targets coupled with a protection velocity limit. Substituting the linear motion equations shown in Equations (1) and (2) arrives at Equation (3). If a target floor acceleration is established and a protection velocity target known, the required floor stroke can be calculated using Equation (3). An additional safety factor was applied and EA component targets were to absorb at least 150% of the primary calculated energy before EA device failure. This resulted in approximately 150mm travel for the constant force EA device. This energy absorbing stroke space claim methodology provided an excellent start point for the more detailed studies and held up throughout the CAMEL program.

Position – acceleration – time relationship

$$d = \frac{1}{2}at^2 \quad (1)$$

Velocity - acceleration – time relationship

$$t = \frac{v}{a} \quad (2)$$

Position – velocity - acceleration relationship

$$d = \frac{v^2}{2a} \quad (3)$$

The second level of EA performance target setting included dynamic testing in the form of a triangular acceleration pulse as generated by a drop tower. Targets were set for area under the curve before failure on both classes of EA devices. Deviation limits were set on the constant force EA device. Force limits were set for the variable force EA device. These were quantified with FEA and component testing.

The third level of EA performance target setting involved considerations for extraneous loads imparted to the floor system during a blast event. These were seen in both vehicle blast simulations and survivability blast testing. The hull walls resonate significantly during a blast event. This creates an arduous environment for the in-plane floor support devices. Although total impulse and energy transfer can be similar, the vehicle hull system acceleration inputs greatly exceed the triangle pulse's peak, requiring component force levels to be determined through explicit FEA. The hull introduces up and down motions as well, which could potentially damage and fail an EA device during a single blast event due to extremely low-cycle fatigue.

Device tolerance to the blast environment nuances and reversals were predominantly evaluated using explicit FEA and advanced material damage accumulation models. Models were evaluated to confirm sufficient safety factor of the EA device material fracture limits during their usage. The entire floor system was also evaluated with the target of reusability and only minor local yielding experienced. Laboratory testing was also performed on pre-damaged parts to verify their tolerance and performance with extra plastic deformation and local gouges and scratches.

The fourth and final level of EA performance targets were generated as full scale testing occurred and variable charge locations were tested. The testing began with impulse levels that were easily managed within the available floor travel. As less favorable charge locations were tested, velocity increased to near the intended maximum system tolerance and stroke envelope. By this point there were already well correlated models to both scaled and full-scale testing. These were used as validation models to confirm the system would be able to protect in the more adverse situations as

well as make minor tweaks to EA device tuning (blast mats only).

DETAILED SIMULATION AND TESTING

The initial floor system development strategy included two separate floor vertical EA profile strategies. A constant force EA device competed against a variable force EA device. The base design concepts were down selected from a trade study and their development was followed from initial design concept through full scale survivability blast testing. Two characteristically differently behaved designs were chosen to minimize risk based on unknowns and allow lessons learned through the development to influence choices without starting over. Aside from the tension shape profile differences, the constant force EA device's design is such that it delivers a considerably lower force in compression due to buckling. Low compression force is important because of its ability to reduce floor accelerations while the hull is resonating throughout the blast event, in parallel with reducing the concerns of low cycle fatigue. The variable force EA device on the other hand, maintained similar compression and tension rates

The constant force EA device began in the form of a tension rod that evolved into a tension tube. Nonlinear finite element analysis was employed to determine EA behavior under tension and the combined effects of geometric deformation and material hardening curves. In the case of the utilized 304 stainless steel, its tensile hardening curve matches the material thinning nicely and results in a gently ramping force vs displacement response seen in Figure 5.

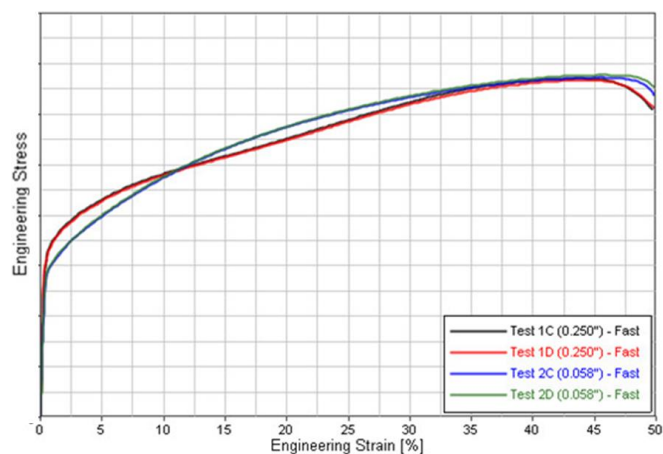


Figure 5: Flat sample 304 stainless stress-strain data

The constant force EA device employs a simple round geometry. The cross-sectional area is tuned to achieve the desired limiting force. As diameters became increasingly small the design was changed to a tubular section to afford enough buckling strength to survive road load requirements.

The geometry utilized is shown in Figure 6 and very similar to a round tensile test sample. This design utilizes a minimal packaging space, narrowly surrounding each seat.



Figure 6: Tension tube assembly

The variable force EA device utilizes a combination of geometric deformation and material hardening curve to achieve a ramped EA profile. The component is created by bolting together a pair of c-shaped pieces to form a ‘double c-damper’ shape. The single c-shape shown in Figure 4 must have its ends supported from in-plane rotation to achieve the required road load strength in combination with the desired EA force profile. This was accomplished by bolting two units facing opposing directions and provided the advantage of an EA device that shrinks in footprint as it narrows while it stretches. Also made using 304 stainless steel, its tensile force-displacement response can be seen in Figure 7 along with the tension tube force-displacement response. The initial strength point is similar between the two types of vertical EA devices to survive road loads.

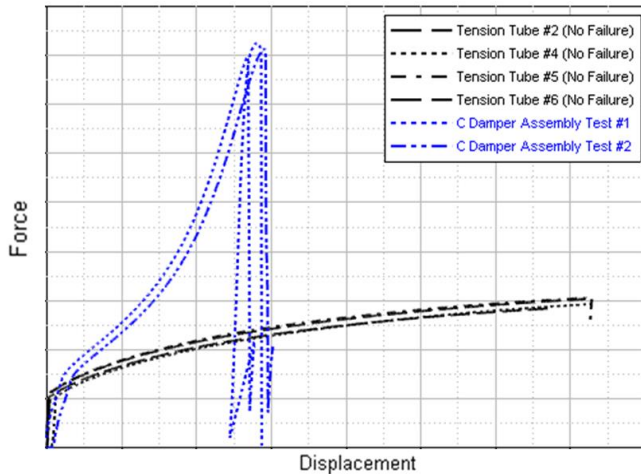


Figure 7: C-damper and tension tube force-displacement response

Early simulations showed the double c-dampers would not be able to survive road loads without additional in-plane support, so their implementation involved swivel joints at each end, similar to the tension tubes. In the CAMEL environment, they consumed more usable space than the tension tubes. The tested design is shown in Figure 8.

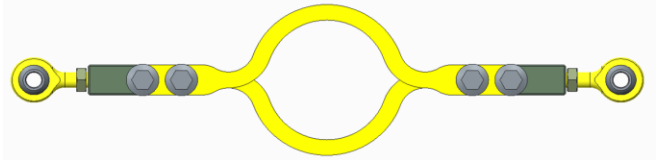


Figure 8: Double c-damper assembly

Component robustness during fielded usage was also paramount for real-world usage. This was a particular concern for the tension tubes. Simulations showed a relatively mangled part would still perform as intended. A test part was created by purposefully damaging a clean piece with bending, scraping, and denting. Gripping implements like pliers were not allowed in the damaging process, but tools like screwdrivers and similar gouging-generating devices were applied. The level of damage involved multiple, purposeful actions and the resulting component performance was effectively equivalent to a virgin test sample. The damaged test piece performance and four other virgin test samples are shown in Figure 9. Physical robustness of the double c-damper was not a concern and consequently not tested.

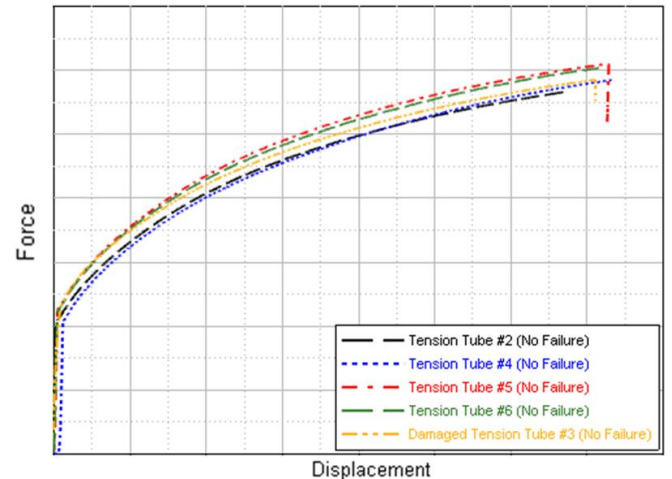


Figure 9: Blemished tension tube performance

The road to first prototype hardware began with a detailed design and analysis process. Components development relied heavily on the use of implicit and explicit FEA. All design details were driven by FEA response. The first prototype hardware dynamic tests involved energy absorption during a 0.4kJ drop test. This process verifies the model accuracy over a range of strains and strain rates. This testing was performed in-house at Pratt & Miller. Data was gathered on impact mass acceleration and maximum travel. Shear panel performance is shown in Figure 10 and the test

part vs FEA end of test shapes are shown in Figure 11. Tension rod drop test performance is shown in Figure 12.

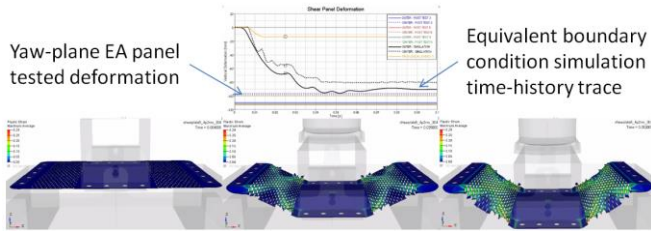


Figure 10: Yaw-plane EA shear panel drop test and simulation

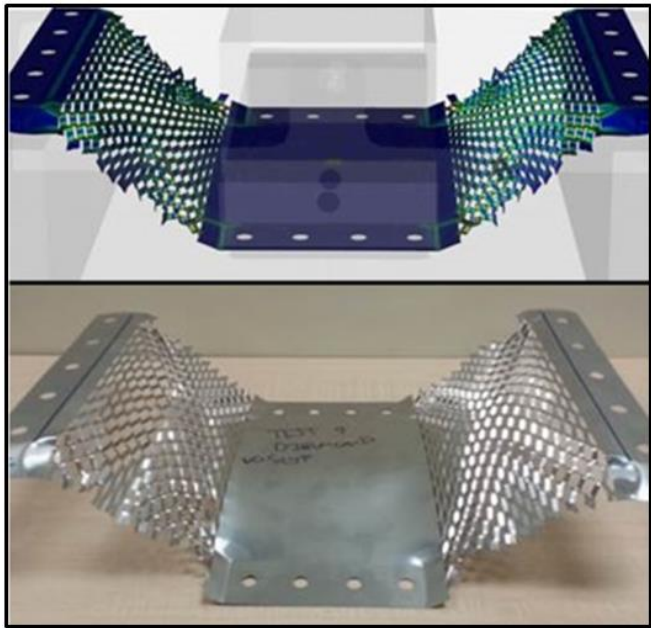


Figure 11: Yaw-plane EA shear panel simulation and test final shape

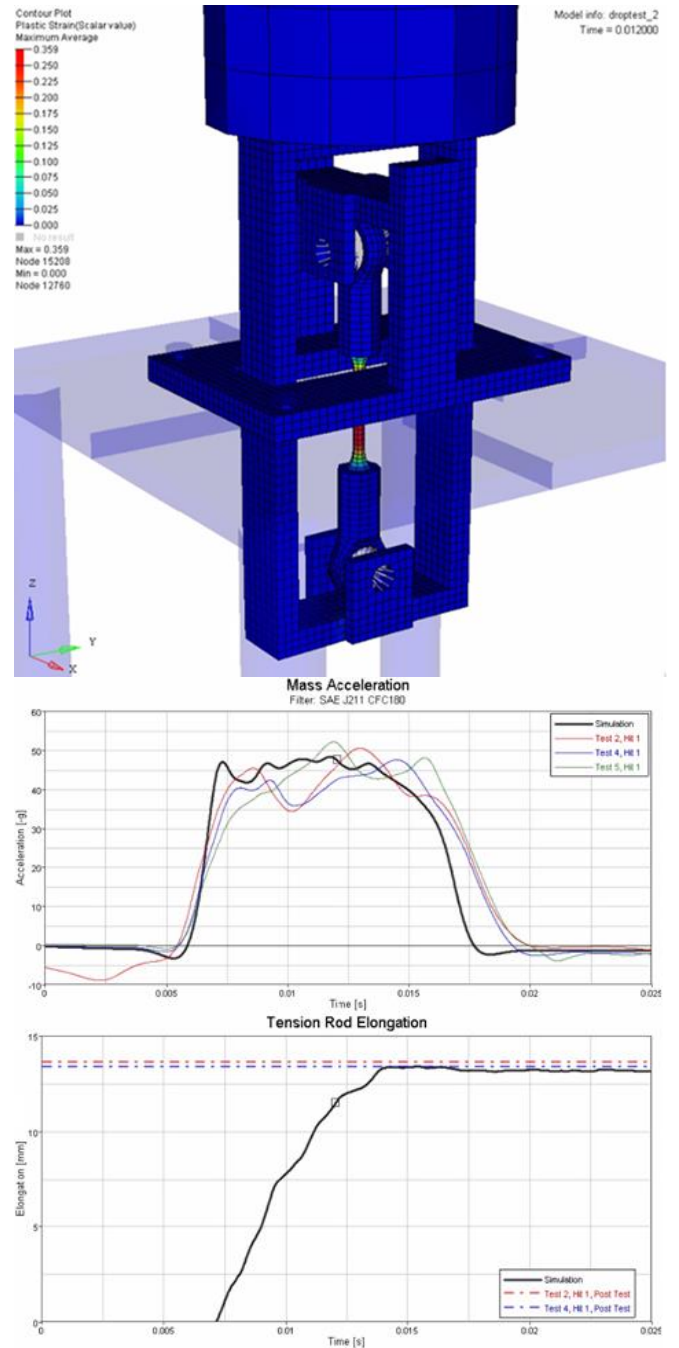


Figure 12: Tension rod drop test and simulation

Tension rods were also tested in tension out to fracture. This was performed to verify robustness and material consistency. The tested 304 stainless steel always exceeded the specified minimum elongation, which is stated as low as 40% from some manufacturers. Data is shown in Figure 13. Components were designed to the minimum elongation and a comfortable safety factor to fracture was achieved. This

material would be a poor choice if an application required fracture after a specific energy absorption.

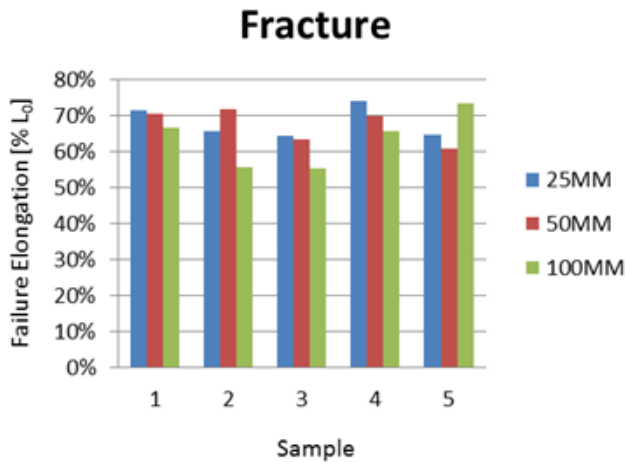


Figure 13: Tension rod drop test to fracture results

After successful dynamic testing was performed and correlated, parts were released for multiple stages of blast testing. This began with low impulse testing using scaled components that were supporting scaled masses. The scaled EA devices were subjected to the same impulse, and featured different active energy absorbing section details. The purpose of this was to validate the modeling methodology, particularly strain and strain rate response curves, and to verify dynamic material elongation limits. The scaled EA devices were run at different geometry to verify performance over a representative envelope.

The thicknesses of the double c-dampers were varied to accomplish different force-displacement results. Sample geometry is shown in Figure 14 including both the pre-test c-shaped sample and the straightened post-test samples. Performance simulation and test results, reported as supported mass acceleration, are shown in Figure 15. The finite element models were a little stronger than the real parts in this case, but general behavior was similar and the peak acceleration values were relatively close.



Figure 14: Scaled double c-dampers pre and post-test

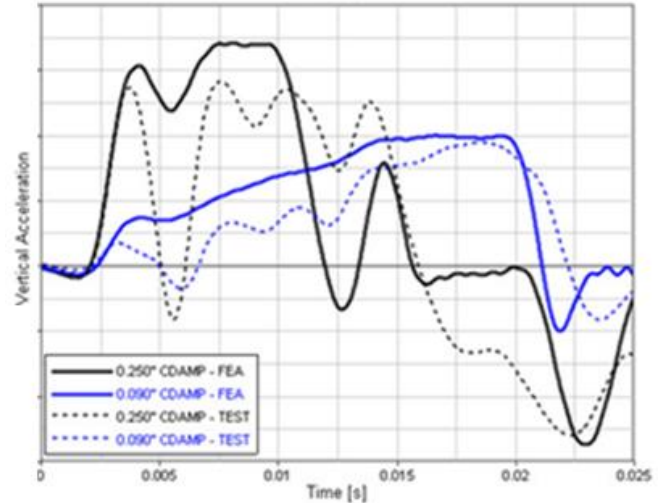


Figure 15: Scaled double c-damper acceleration correlation

The length of the tension rod was varied to obtain a material performance map. As length decreases, both the strain and strain rate increase. Test tension rods are shown in Figure 16. Note the black finish was a consequence of a specific vendor processing and later components did not have this appearance. This results in a stiffer response with a shorter sample, as seen in both test and simulation in results in Figure 17. The correlation between test and simulation was very good.



Figure 16: Scaled tension rods pre and post-test

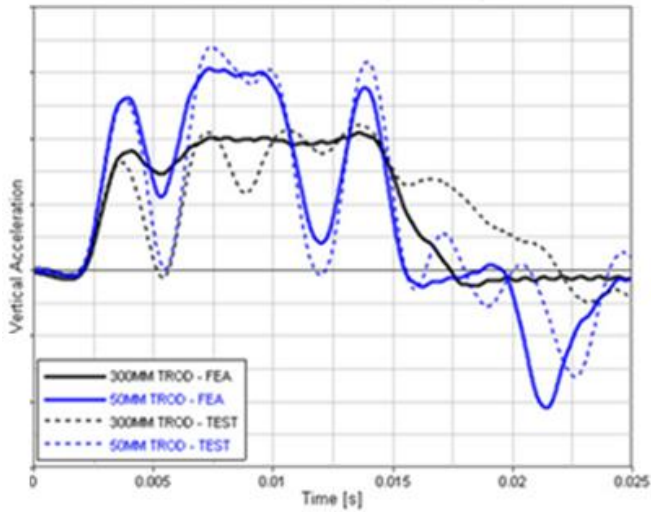


Figure 17: Scaled tension rod acceleration correlation

Scaled yaw-plane EA shear panels were tested for vertical performance. They supported a mass alone in this test, without any vertical EA devices. The purpose of this test was to verify their system-level contribution to vertical EA behavior. The test components are shown in Figure 18, and good agreement between simulated and tested acceleration is shown in Figure 19.

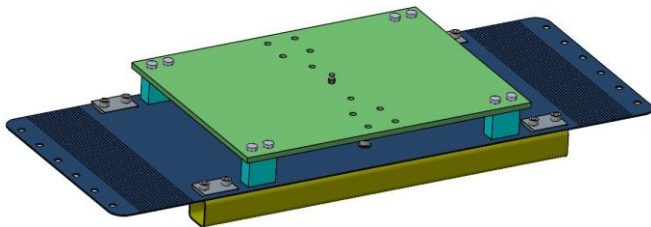


Figure 18: Scaled yaw-plane EA shear panel

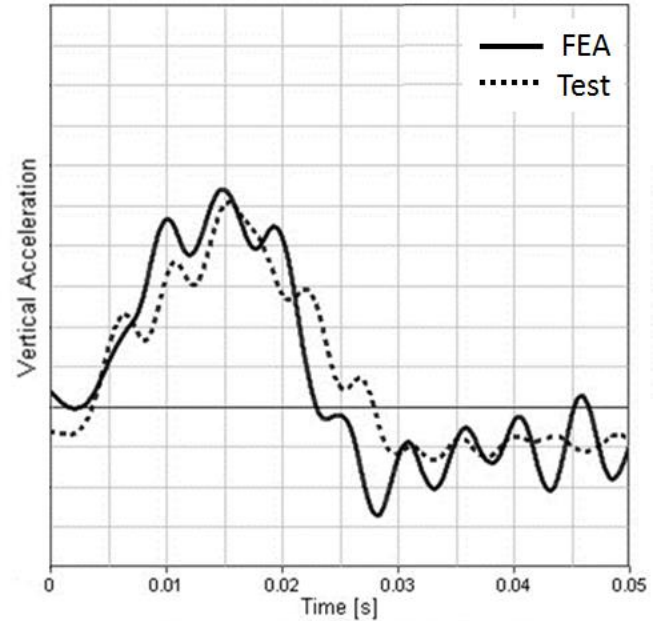


Figure 19: Scaled yaw-plane EA shear panel acceleration correlation

The next step included full-sized system tests, but with test masses on the floor system rather than a complement of ATDs and seats to minimize potential risks. Architecture and test setup are shown in Figure 20. These tests featured two floor systems, one with the double c-damper vertical EA and the other with the tension tube vertical EA. All tested floor systems utilized shear panels for yaw-plane support. The two larger footprint masses per station mounted outboard represented seat and occupant mass contributions to the floor response. The four smaller masses per station located along the centerline were meant to represent foot loading to the floor system. This test added the complexity of a full floor system's elastic response as well as a blast mat.

The system structure was fully modeled in LS-DYNA with the blast mat included. The blast mat model included fully detailed compression-force response with strain rate sensitivity over the pertinent range. Floor and test mass accelerations were monitored along with loads at the vertical EA mount locations. The vertical EA instrumentation is shown in Figure 21.

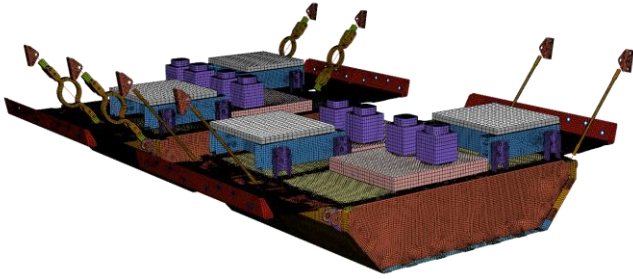


Figure 20: Full-sized system model with test masses

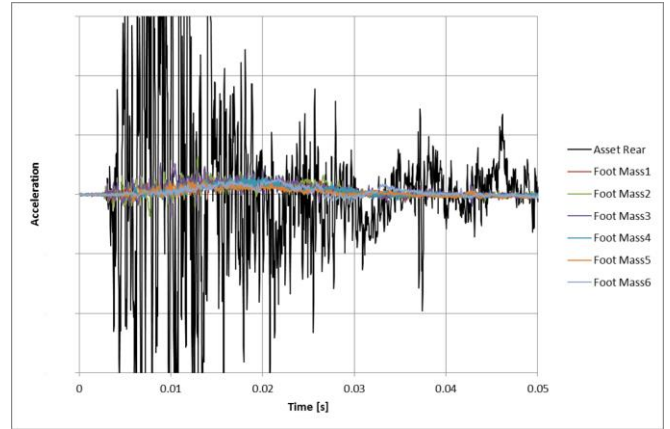


Figure 22: Full-sized system with leg masses response



Figure 21: Vertical EA force instrumentation

The hull and leg mass test responses are shown in Figure 22. This shows the significance of the full floor system. Although bulk acceleration and velocity build of the entire floor system remains similar to the hull as shown in Figure 23, the acceleration response the foot masses experience is dramatically less active. The floor system vertical EA does the majority of the acceleration pulse shaping, leaving just some high frequency noise fed through mostly individual floor panel modes. The blast mat is highly effective in negating these local oscillations, acting as a light-weight low pass filter.

The conclusion of full sized system testing marked the required timeline to perform the vertical EA device down-select. Both the double c-damper and tension tube designs showed excellent performance potential. Both floors achieved significant peak velocity reduction compared to the hull, with the tension tube floor performing slightly better. The double c-damper vertical EA device system also showed a sharp decrease in velocity and more velocity change (energy input) due to transmitting compression loads more effectively than the tension tube floor at about 20-30ms as seen in Figure 23. The slightly improved performance combined with considerably better packaging in the CAMEL environment drove the choice to proceed with tension tubes vertical EA devices in subsequent CAMEL design and test activities.

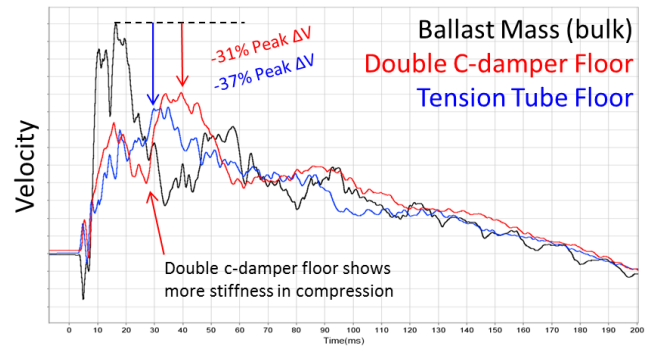


Figure 23: Full-sized tension tube and c-damper floor system velocity response during blast testing

After performance and correlation in the proof of concept tests was completed, additional detail was added to properly capture the foot and tibia response. Occupant modeling began much earlier in parallel with the scaled full-sized system models using the LSTC Fast ATD models. These ATD models have repeatedly proved to provide accurate structural loading and basic response. To achieve the

fidelity required for injury prediction, the LSTC Detailed ATD models were utilized. The ATD models were modified by adding slider gear and clothing. This included separate models for the 5th, 50th, and 95th percentile test models. The appropriate boot characteristics are particularly significant for tibia load accuracy. Common boot sizes for each ATD were modeled and implemented. Boot sole EA characteristics were also measured; appropriate energy-absorbing strain and strain-rate sensitive material models were utilized. While repeated cycles showed some EA performance changes at both the boot soles and blast mats, fortunately these effects were not large enough to significantly alter system performance.

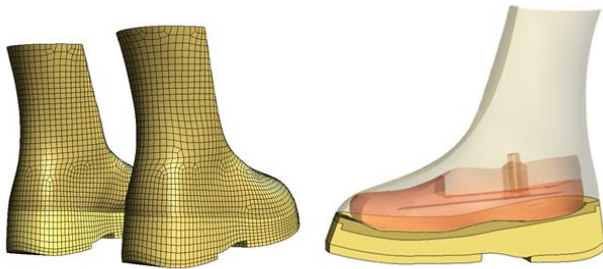


Figure 24: Detailed ATD boot model

With the floor system bulk response during a blast event well tested and modeled, focus shifted to the foot to tibia response. Tibia response correlation data generation was piggybacked with seat drop tower testing. The seat test series focused on the floor-mounted seats and the input was designed to mimic the floor response.

The first boot and ATD model correlation was performed to legacy drop tower test data without a blast mat. The early Fast ATD models loaded too quickly, but detailed ATD and boot models fixed the phasing. While peak loads were slightly under-predicted, the phasing was deemed more appropriate to correlate in this non-representative environment. Peak load agreement was more scrutinized with the blast mats included and when injury was a concern. Model responses are shown in Figure 25.

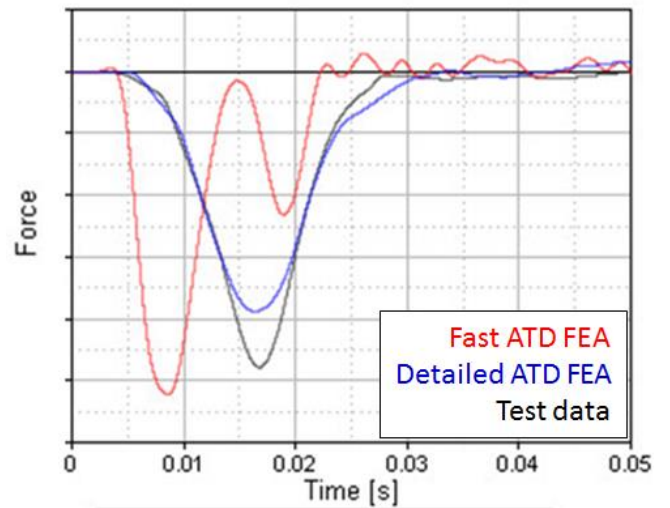


Figure 25: Tibia drop tower - 5th ATD at 2.5m/s no blast mat

Drop tower tests were mainly performed with the 5th percentile ATD and the most statistically robust tibia response data comes from this arrangement. Tests were performed up to 6m/s velocity. As more detail was verified and added to the model, timing and peak value correlation was improved. These gains were all accomplished by adding test details, not by adjusting responses. The load ramp rate was highly dependent on material properties. The timing of the event was influenced by any air gap between the boot and the mat before impact. The final result has the FEA model following timing trends well and slightly under-predicting lower tibia load in a low intensity event (Figure 26), while delivering accurate results in a high intensity event (Figure 27).

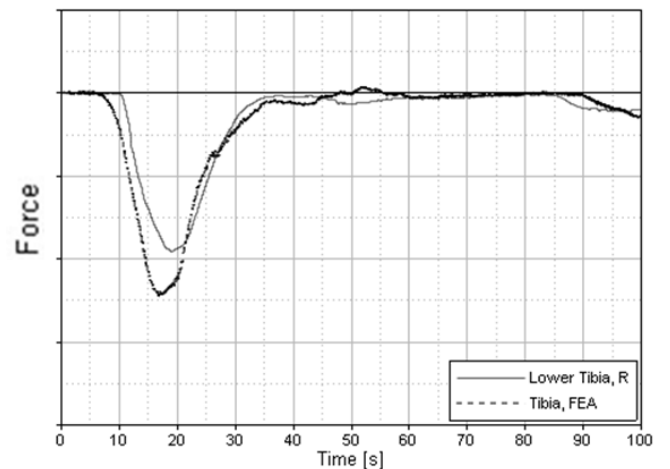


Figure 26: Drop tower tibia load correlation using blast mat and 3.5m/s delta-V

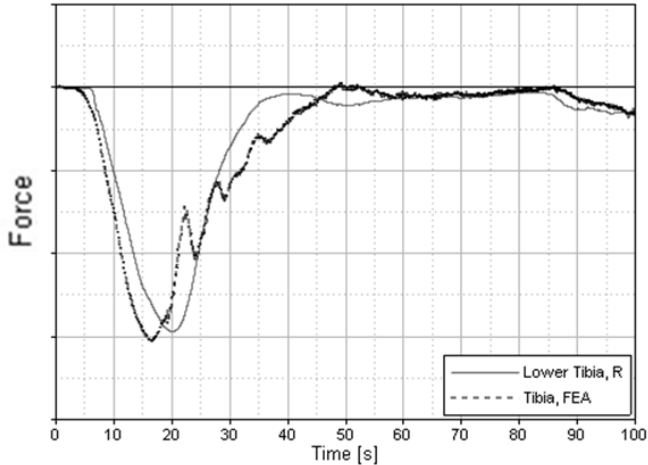


Figure 27: Drop tower tibia load correlation using blast mat and 6.0m/s delta-V

The final test stages involved multiple full assets undergoing blast survivability testing with bucks growing in complexity all the way to having suspension and wheels. These were loaded with a full complement of ATDs and 5-9 station floor systems. Purposefully injury-challenging ATD layouts were selected to test worst-case survivability performance.

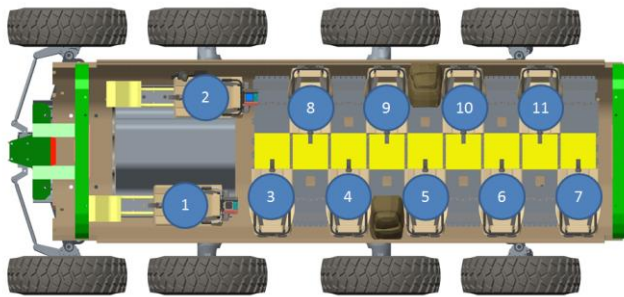


Figure 28: ATD placement in test asset

Multiple tests were performed and room for improvement was identified in analysis by utilizing a slightly softer tuned blast mat because the injury values were approaching limits. Softening the blast mat must be done cautiously to avoid system response overshoot. Correlation remained very good though this change and in all tests overall. The blast pulse increased slightly from mid-program expectations to approximately the original design velocities after the worst case blast location simulations were completed.

Detailed occupant pre-test predictions were performed in all cases where levels of risk were suspected to be high due to either charge location or a change in the asset. When the asset was configured as-shown in Figure 28 and the charge placed at the rear for the CDR1 test, a complete pre-test

prediction was performed for each occupant. The full 9-station LS-DYNA floor model is shown in Figure 29. No lower extremity injury was experienced and the results were compared to the pre-test predictions. Those results agreed quite well, as shown in Figure 30 and for occupant locations as detailed in Figure 28.

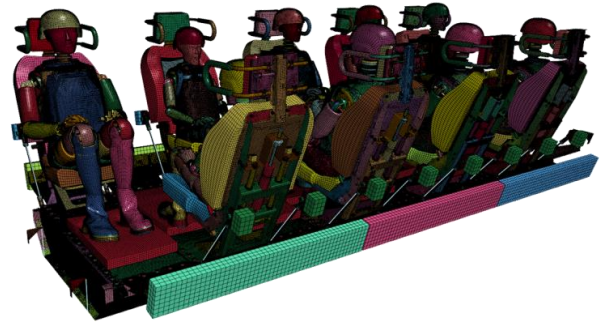


Figure 29: 9-station floor LS-DYNA model

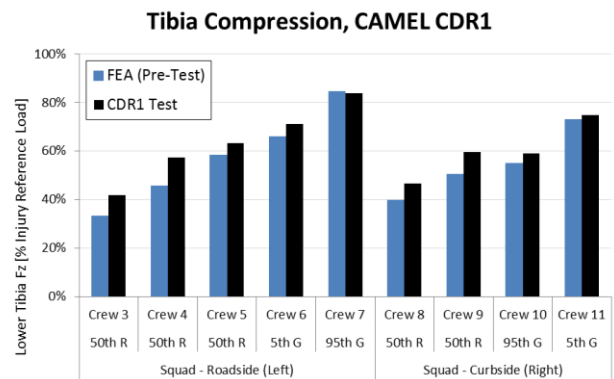


Figure 30: CDR1 tibia load test & pre-test FEA

Detailed tibia time-history correlation plots for high and low intensity inputs as well as all utilized ATD sizes are shown in Figure 31, Figure 32, and Figure 33. The pre-test floor system performance predictions used full vehicle simulation inputs. Even with slight input differences between simulation and blast survivability testing, the time-history correlation is generally very good.

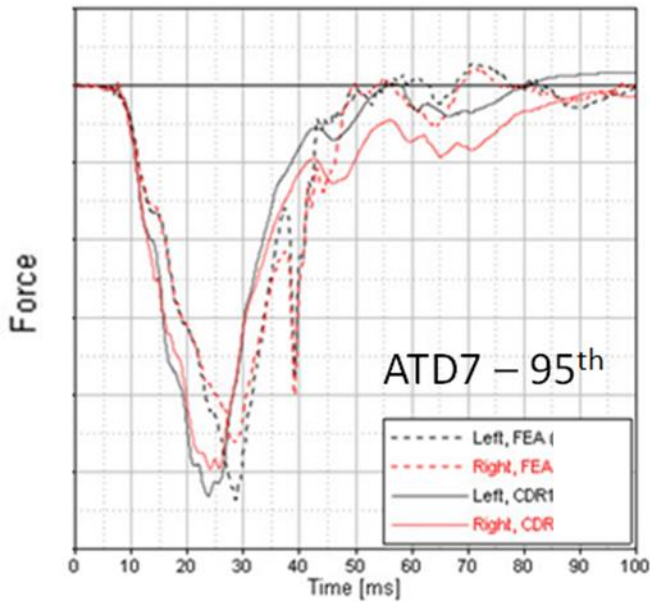


Figure 31: Full asset blast testing - 95th percentile ATD high intensity input correlation

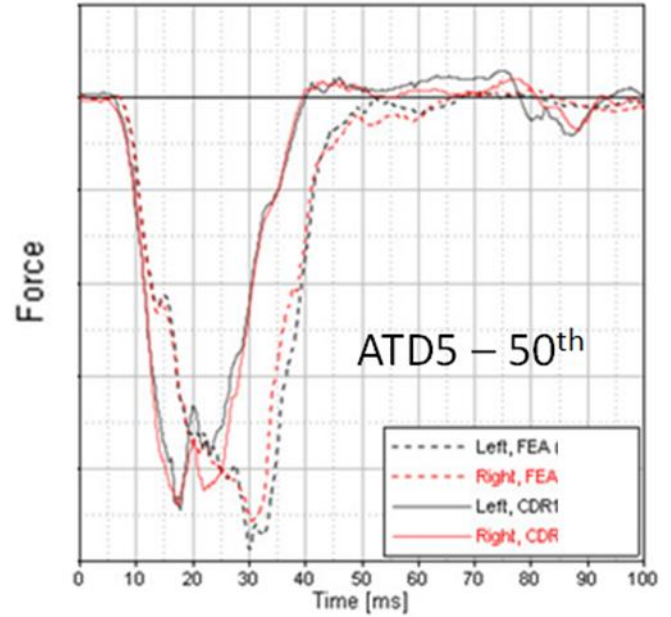


Figure 33: Full asset blast testing - 50th percentile ATD low intensity input correlation

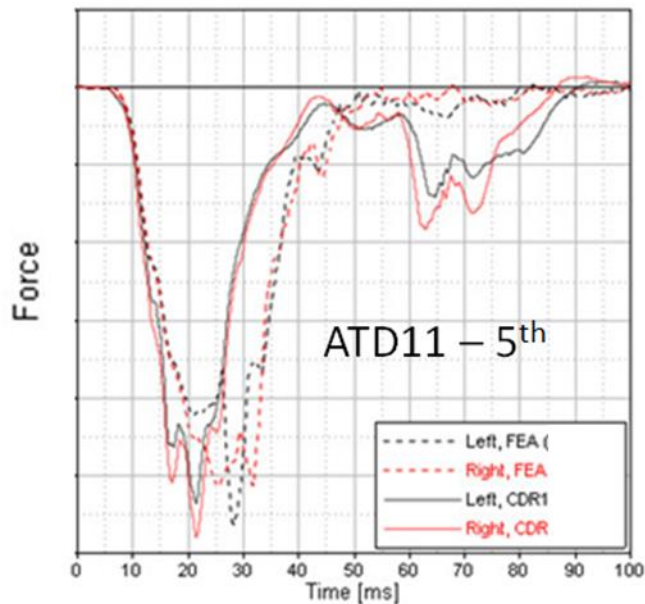


Figure 32: Full asset blast testing - 5th percentile ATD high intensity input correlation

Floor stroke was instrumented to verify travel during an event. In the worst case events, approximately 85mm of peak travel was utilized, including elastic overshoot. Floor stroke varies proportional to event severity and one end of the floor can stroke more or less than the other based upon local severity. Rear corner of floor travel vs time from a rear charge location can be seen in Figure 34. Slight differences in asset velocity were noted from simulation to test, accounting for the stroke mismatch. The general behavior and motion is a good match.

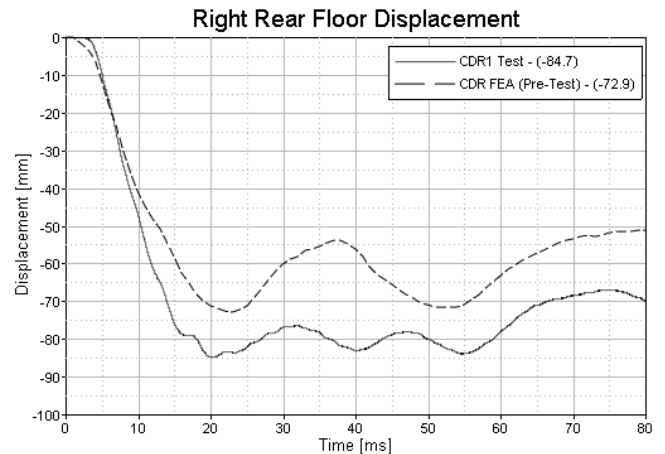


Figure 34: Floor stroke test and simulation

Throughout the CAMEL program the floor system was subjected to a wide range of charge inputs from end to end and event to event. Charges were also placed off-center to test lateral and rotational effects. There was significant impulse change for multiple occupants with different charge locations, providing a thorough floor performance mapping from low through high intensity events. The largest range was provided with rear-positioned charges which involved a large range of asset pitch and varied from high velocity at the rear to nearly zero velocity at the front of the floor. Excellent injury mitigation was observed over the entire test series. The system test performance map is shown in Figure 35.

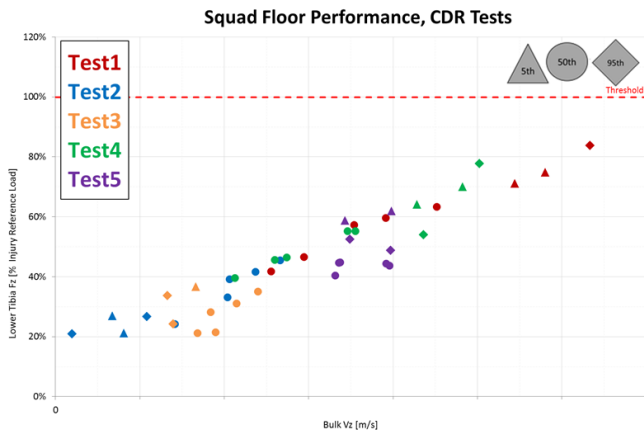


Figure 35: Floor system performance map



Figure 36: Test asset with full ATD load

CONCLUSIONS

The CAMEL program was tasked with solving the challenging problem of mitigating lower extremity injury from the 5th, 50th, and 95th percentile ATDs during center and offset blast locations in tandem with creating a feasible

occupant concentric vehicle. The tradeoffs between EA performance, occupant centric, and warfighter packaging requirements were balanced to create an innovative solution that sets precedent for future blast mitigation programs.

The CAMEL program developed a simple and feasible passive system that limits the blast energy directed into the floor system. The floating floor system mitigated the severe resonating force of the hull during the blast event by systematic component placement and by buckling the EA devices in compression. The constant force solution solved the occupant loadout problem by maintaining a high floor system mass, reducing the significance of each occupant's mass contribution.

The floor system was thoroughly tested from a lab environment all the way through full scale survivability blast testing. Twelve full scale blast tests were performed and over seventy full-instrumented ATDs all showed zero lower-extremity injuries. The floor system is also reusable by replacing the EA devices, multiple floor base structures were reused during survivability blast testing with only the intended EA service performed. The final solution is a simple, low-cost, sustainable floor system that can protect the warfighter at very high blast levels.

The CAMEL program floor system development process concluded not just with a floor system that performed well in all tested and simulated conditions, but included a fundamental understanding of the acceleration limit and impulse application control necessary to protect our warfighter. This process developed a fine level of insight to all facets of the current system's performance and also allows for future improvements in other occupant protection systems. Successful correlation of all systems responses stemmed from solid base physics along with detailed correlation on each individual component's contribution. This fully detailed approach captured many nuances that simplified modeling would have missed, such as local floor panel modes, wall resonances, and EA device reverse loads. The methodology has uncovered and developed the critical performance characteristics along with providing insight to further improve performance by utilizing less stroke and packaging space.

Reference herein to any specific commercial company, product, process, or service by trade name, trademark, manufacturer, or otherwise does not necessarily constitute or imply its endorsement, recommendation, or favoring by the United States Government or the Dept. of the Army (DoA). The opinions of the authors expressed herein do not necessarily state or reflect those of the United States Government or the DoD, and shall not be used for advertising or product endorsement purposes.

REFERENCES

[1] Vasquez K, Logsdon K, Shivers B, Chancey C. Medical Injury Data 10 Nov 2011.
http://www.ircobi.org/downloads/irc13/pdf_files/24.pdf

[2] S. Desjardins “The Evolution of Energy Absorption Systems for Crashworthy Helicopter Seats”, Safe Inc., 2003